Precision Measurements of the Λ_c^+ and D^0 Lifetimes

A. Kushnirenko,[3] G. Alkhazov,[11] A. G. Atamantchouk,[11] M. Y. Balatz,[8,a] N. F. Bondar,[11] P. S. Cooper,[5] L. J. Dauwe,[17]
G. V. Davidenko,[8] U. Dersch,[9,b] A. G. Dolgolenko,[8] G. B. Dzyubenko,[8] R. Edelstein,[3] L. Emediato,[19] A. M. F. Endler,[4]
J. Engelfried,[13,5] I. Eschrich,[9,c] C. O. Escobar,[19,d] A. V. Evdokimov,[8] I. S. Filimonov,[10,a] F. G. Garcia,[19,5] M. Gaspero,[18]
I. Giller,[12] V. L. Golovtsov,[11] P. Gouffon,[19] E. Gülmez,[2] He Kangling,[7] M. Iori,[18] S. Y. Jun,[3] M. Kaya,[16] J. Kilmer,[5]
V. T. Kim,[11] L. M. Kochenda,[11] I. Konorov,[9,e] A. P. Kozhevnikov,[6] A. G. Krivshich,[11] H. Krüger,[9,f] M. A. Kubantsev,[8]
V. P. Kubarovsky,[6] A. I. Kulyavtsev,[3,g] N. P. Kuropatkin,[11] V. F. Kurshetsov,[6] S. Kwan,[5] J. Lach,[5] A. Lamberto,[20]
L. G. Landsberg,[6] I. Larin,[8] E. M. Leikin,[10] Li Yunshan,[7] M. Luksys,[14] T. Lungov,[19,h] V. P. Maleev,[11] D. Mao,[3,g]
Mao Chensheng,[7] Mao Zhenlin,[7] P. Mathew,[3,i] M. Mattson,[3] V. Matveev,[8] E. McCliment,[16] M. A. Moinester,[12]
V. V. Molchanov,[6] A. Morelos,[13] K. D. Nelson,[16,j] A. V. Nemitkin,[10] P. V. Neoustroev,[11] C. Newsom,[16] A. P. Nilov,[8]
S. B. Nurushev,[6] A. Ocherashvili,[12] Y. Onel,[16] E. Ozel,[16] S. Ozkorucuklu,[16] A. Penzo,[20] S. V. Petrenko,[6] P. Pogodin,[16]
M. Procario,[3,k] V. A. Prutskoi,[8] E. Ramberg,[5] G. F. Rappazzo,[20] B. V. Razmyslovich,[11] V. I. Rud,[10] J. Russ,[3]
P. Schiavon,[20] J. Simon,[9,l] A. I. Sitnikov,[8] D. Skow,[5] V. J. Smith,[15] M. Srivastava,[19] V. Steiner,[12] V. Stepanov,[11]
L. Stutte,[5] M. Svoiski,[11] N. K. Terentyev,[11,3] G. P. Thomas,[1] L. N. Uvarov,[11] A. N. Vasiliev,[6] D. V. Vavilov,[6]
V. S. Verebryusov,[8] V. A. Victorov,[6] V. E. Vishnyakov,[8] A. A. Vorobyov,[11] K. Vorwalter,[9,m] J. You,[3,5] Zhao Wenheng,[7]
Zheng Shuchen,[7] and R. Zukanovich-Funchal[19]

(SELEX Collaboration)

[1]*Ball State University, Muncie, Indiana 47306*
[2]*Bogazici University, Bebek 80815 Istanbul, Turkey*
[3]*Carnegie-Mellon University, Pittsburgh, Pennsylvania 15213*
[4]*Centro Brasileiro de Pesquisas Físicas, Rio de Janeiro, Brazil*
[5]*Fermilab, Batavia, Illinois 60510*
[6]*Institute for High Energy Physics, Protvino, Russia*
[7]*Institute of High Energy Physics, Beijing, Peoples Republic of China*
[8]*Institute of Theoretical and Experimental Physics, Moscow, Russia*
[9]*Max-Planck-Institut für Kernphysik, 69117 Heidelberg, Germany*
[10]*Moscow State University, Moscow, Russia*
[11]*Petersburg Nuclear Physics Institute, St. Petersburg, Russia*
[12]*Tel Aviv University, 69978 Ramat Aviv, Israel*
[13]*Universidad Autónoma de San Luis Potosí, San Luis Potosí, Mexico*
[14]*Universidade Federal da Paraíba, Paraíba, Brazil*
[15]*University of Bristol, Bristol BS8 1TL, United Kingdom*
[16]*University of Iowa, Iowa City, Iowa 52242*
[17]*University of Michigan-Flint, Flint, Michigan 48502*
[18]*University of Rome "La Sapienza" and INFN, Rome, Italy*
[19]*University of São Paulo, São Paulo, Brazil*
[20]*University of Trieste and INFN, Trieste, Italy*
(Received 6 October 2000)

We report new precision measurements of the lifetimes of the Λ_c^+ and D^0 from SELEX, the charm hadroproduction experiment at Fermilab. Based upon 1630 Λ_c^+ and 10 210 D^0 decays we observe lifetimes of $\tau[\Lambda_c^+] = 198.1 \pm 7.0 \pm 5.6$ fs and $\tau[D^0] = 407.9 \pm 6.0 \pm 4.3$ fs.

Lifetime measurements of the charm baryons help to determine the contributions of non-spectator weak interaction effects like W-annihilation and W-exchange processes without the helicity suppression that limits their role in charm meson decays. From the point of view of heavy quark effective theory and perturbative QCD, the charm baryon lifetimes can be expressed in terms of a set of matrix elements that contain the corrections to the fundamental expansion of the decay amplitude in terms of $1/m_c$ [1–3]. The Λ_c^+ lifetime is the best measured

of the four stable charm baryons [4]. We present a new measurement from hadro-production data taken by the SELEX(E781) [5] experiment at Fermilab. Using the same data sample, cuts, and techniques, we have also measured the lifetime of the D^0 with a precision comparable to the best present measurements [4]. This new D^0 measurement verifies our lifetime analysis procedure in a sample with higher statistical precision and larger corrections than the Λ_c^+. Details may be found in Ref. [6].

The SELEX experiment uses the Fermilab charged hyperon beam at 600 GeV to produce charm particles in a set of thin foil targets of Cu or diamond. The three-stage magnetic spectrometer is shown elsewhere [5,6]. The most important features for the charm lifetime studies are the high-precision vertex detector that provides an average proper time resolution of 20 fs for the charm decays, a 10 m long Ring-Imaging Cerenkov (RICH) detector that separates π from K up to 165 GeV/c [7], and a high-resolution tracking system that has momentum resolution of $\sigma_p/p < 1\%$ for a 200 GeV/c reconstructed Λ_c^+. Figure 1 shows the vertex region in detail with an overlay of reconstructed tracks, error corridors, and measured parameters for a clear Λ_c^+ event.

The experiment selected charm candidate events using an online secondary vertex algorithm. A scintillator trigger demanded an inelastic collision with at least four charged tracks in the interaction scintillators and at least two hits in the positive particle hodoscope after the second analyzing magnet. Event selection in the online filter required full track reconstruction for measured fast tracks ($p \gtrsim 15$ GeV/c). These tracks were extrapolated back into the vertex silicon planes and linked to silicon hits. The beam track was measured in upstream silicon detectors. A full three-dimensional vertex fit was then performed. An event was written to tape if all the fast tracks in the event were *inconsistent* with having come from a single primary vertex. This filter passed 1/8 of all interaction triggers and had about 50% efficiency for otherwise accepted charm decays. The experiment recorded data from 15.2×10^9 inelastic interactions and wrote 1×10^9 events to tape using both positive and negative beams. 65% of events were Σ^- induced with the balance split roughly equally between π^- and protons.

The analysis selected charm events with a topological identification procedure. Only charged tracks with re-
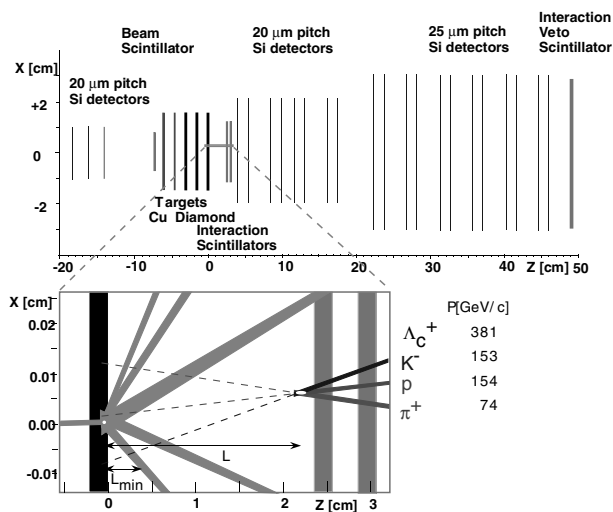
constructed momenta were used. Tracks which traversed the RICH ($p \gtrsim 22$ GeV/c) were identified as protons or kaons if those hypotheses were more likely than the pion hypothesis. All other tracks were assumed to be pions. The primary vertex was refit using all found tracks. An event was rejected if all the tracks were consistent with only a primary vertex. For those which were inconsistent, secondary vertices were formed topologically. Charm candidates were selected if the secondary decay tracks satisfied requirements on effective mass (200 MeV window), K/p particle identification (RICH) and correct net charge for a given charm state.

The charm decay modes used were $\Lambda_c^+ \rightarrow pK^-\pi^+$ and $D^0 \rightarrow K^-\pi^+$, $K^-\pi^+\pi^-\pi^+$ + charge conjugate. No $\overline{\Lambda}_c^-$ candidates were considered because of the strong production asymmetry in this data sample. The charm event selection criteria required: (i) acceptable fits for all tracks and vertices, (ii) all track momenta exceed 8 GeV/c, (iii) proton and kaon tracks to be RICH identified, (iv) the secondary vertex to reconstruct upstream of the interaction counters and at least 0.5 mm from any target or other material, (v) the significance of the primary-secondary vertex separation, L, be at least 8σ, where σ is the error on L, (vi) σ to be less than 1.7 mm, (vii) two charm decay tracks with miss distances to the primary vertex greater than 20 μm in space, (viii) and the charm momentum be parallel to the vector from primary to secondary vertex within errors. The mass peaks for the candidate events selected are shown in Fig. 2.

Because the proper time resolution is short compared to the expected Λ_c^+ lifetime of $\sim$200 fs, we use a binned lifetime analysis. We bin in reduced proper lifetime; $t_R = (L - L_{min})M/pc$, where M is the known charm state mass [4], p its reconstructed momentum, L the measured vertex separation, and L_{min} the minimum L for each event to pass all the imposed selection cuts. L_{min} varies event by event. This quantity t_R should have an exponential distribution with the lifetime of the decaying state for acceptance-corrected signal events.
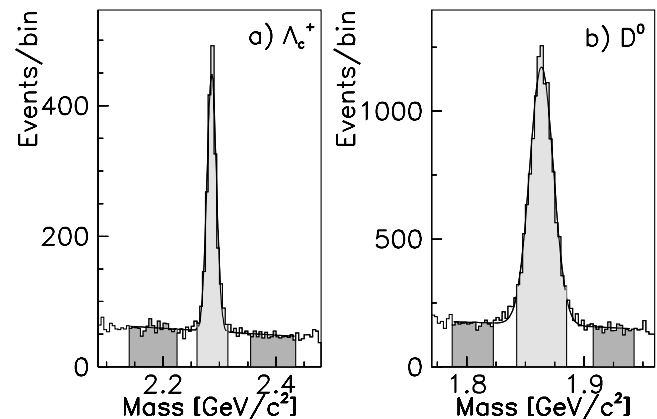

FIG. 1. The charm targets and vertex detector. A clear example of a Λ_c^+ event with track error corridors and vertex error ellipses is shown in the expanded region.

FIG. 2. The mass distribution for the (a) Λ_c^+ sample in 5 MeV/c^2 bins and (b) D^0 sample in 2.5 MeV/c^2 bins. The signal and sideband regions are shaded.

To correct the raw proper time distributions, one must understand the apparatus acceptance as a function of the proper time. Apparatus acceptance for a charm decay at a given proper time depends on global event characteristics, e.g., track multiplicity, momenta, decay configuration, and decay position along the spectrometer axis. A suitable simulation program would not only produce correctly the kinematics of charm pair production, but also have a correct reproduction of the underlying event. Because neither the true distributions of track characteristics in the underlying event nor the true production properties of charm hadrons in our data (momentum, track multiplicities, ...) are known, we decided to evaluate the proper time acceptance for the sample of events *that we actually observe.* In the SELEX apparatus, proper time acceptance depends only on the vertex region detectors, because the downstream detectors are not sensitive to centimeter-scale shifts of the decay vertex. Each event was passed through the reconstruction program multiple times, stepping the charm decay point to different distances L from the primary vertex. Event topology, momenta, and other properties of the global event were kept fixed. At each L this charm event was either rejected or accepted. We also took into account losses due to secondary interactions in the targets. In this way the acceptance of each observed event as a function of

proper time t_R was determined. The overall efficiency of the observed sample is just the weighted average of the individual event efficiencies [6]. This technique preserves the production and acceptance properties and correlations in the data including the underlying event without requiring a complete simulation of charm production.

We make t_R distributions for the signal and sideband regions, shown in Fig. 2. A simultaneous maximum likelihood fit to both the signal $N_s(t_R)$ and sideband $N_b(t_R)$ distributions is made:

$$N_s(t_R) = \frac{N_0}{\tau} e^{-t_R/\tau} \cdot \epsilon(t_R) + C \cdot B(t_R), \qquad (1)$$

$$N_b(t_R) = B(t_R) = \frac{N_1}{\tau_1} e^{-t_R/\tau_1} + \frac{N_2}{\tau_2} e^{-t_R/\tau_2}. \qquad (2)$$

The sideband distribution is represented with a background function $B(t_R)$. The signal distribution is represented with the same background function $B(t_R)$ plus an exponential times acceptance $\epsilon(t_R)$ for the signal. Coefficient C takes into account widths of signal and sideband regions. The acceptance, acceptance-corrected distributions, and fits are shown in Fig. 3.

As a consistency check we have repeated the analysis for each decay mode and for events from each target separately. The acceptance function changes significantly between these cases. The lifetimes from these fits are tabulated in Table I. All the fits have acceptable quality. The independent measurements are consistent with each other and with the global lifetime fit.

We have made a detailed study of systematic effects using the charm data itself, Monte Carlo simulations, and a sample of 2×10^6 observed $K_s^0 \rightarrow \pi^+\pi^-$ decays. The non-negligible contributions are tabulated in Table II. The
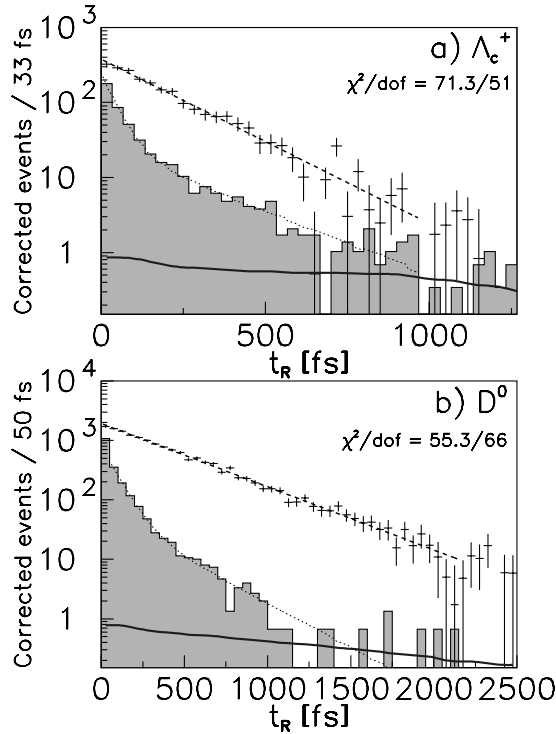

FIG. 3. The acceptance-corrected reduced proper lifetime distributions for the background subtracted signal (points) and sideband (shaded) regions for (a) Λ_c^+ in 33 fs bins and (b) D^0 in 50 fs bins. The dashed line is the lifetime fit. The background is normalized to the width of the signal region shown in Fig. 2. The solid line is the acceptance as a function of t_R. χ^2 represents the result of the binned likelihood fit of signal and background reduced proper time distributions. The fitting function is given by Eqs. (1) and (2).

TABLE I. Complete and subsample lifetimes with statistical errors. The probability of χ^2 to be greater than the observed value is shown in parentheses.

Decay mode	τ (fs)	Events
$D^0 \rightarrow K^-\pi^+$, $K^-\pi^+\pi^-\pi^+$ + c.c.	407.9 ± 6.0	$10\,210 \pm 125$
$\Lambda_c^+ \rightarrow pK^-\pi^+$	198.1 ± 7.0	1630 ± 45
$D^0 \rightarrow K^-\pi^+$	416 ± 12	2470 ± 57
$\overline{D}{}^0 \rightarrow K^+\pi^-$	416 ± 10	3420 ± 65
$D^0 \rightarrow K^-\pi^+\pi^-\pi^+$	399 ± 16	1950 ± 63
$\overline{D}{}^0 \rightarrow K^+\pi^-\pi^+\pi^-$	400 ± 14	2360 ± 66
Average	410.3 ± 6.3	
χ^2/dof (prob)	$1.46/3$ (69%)	

Target	Λ_c^+ τ (fs)	D^0 τ (fs)
1 Copper	198 ± 20	394 ± 13
2 Copper	198 ± 22	422 ± 14
3 Diamond	229 ± 25	413 ± 15
4 Diamond	178 ± 14	412 ± 14
5 Diamond	202 ± 16	413 ± 16
Average	195.2 ± 8.2	410.1 ± 6.4
χ^2/dof (prob)	$3.53/4$ (47%)	$2.20/4$ (70%)

TABLE II.   Systematic error contributions.

	Λ_c^+ $\sigma(\tau)$ (fs)	D^0 $\sigma(\tau)$ (fs)
Acceptance	5.1	3.8
Mass reflections	1.3	$\cdots$
Background systematics	$\cdots$	1.0
Second charm in event	<1.0	<1.0
Other	<1.5	<1.5
Total (quadrature)	5.6	4.3

dominant contribution is the uncertainty in the determination of the acceptance function. This error was based on studies of charm lifetime measurements for different targets, for different momentum ranges, for different event multiplicities, for charm decays in different z regions, for varying sample-defining cuts, and for the use of proper time instead of reduced proper time in the fit.

Many other effects, including mass reflections, effects of the presence of a second charm particle in the event, interaction losses in the targets, backgrounds induced by mismeasurements of charm decays, different fitting techniques, different definitions of minimum distance $L_{\min}$, etc., have been studied. Mass reflections were dominated by $D_s^+ - \Lambda_c^+$ reflection where the K^+ in $D_s^+ \to K^+ K^- \pi^+$ decay was misidentified as a proton. The lifetime change with different choices of sideband regions is negligible. Decay tracks from the second charm particle in the same event can influence the fit of the primary vertex and may lead to an error in the distance L. All small systematic errors were included in the "other" entry of Table II.

Based upon 1630 Λ_c^+ and 10 210 D^0 decays we observe lifetimes of $\tau[\Lambda_c^+] = 198.1 \pm 7.0 \pm 5.6$ fs and $\tau[D^0] = 407.9 \pm 6.0 \pm 4.3$ fs. These results are consistent with the present PDG averages [4]: $\tau[\Lambda_c^+] = 206 \pm 12$ fs and $\tau[D^0] = 412.6 \pm 2.8$ fs. The precision of our $\tau[D^0]$ measurement is within a factor of 2 of the most precise measurements [8–10]. As a final cross check we have applied our analysis to $D^\pm \to K^\mp \pi^\pm \pi^\pm$ where our acceptance corrections are much larger than in these analyses. Our result $\tau[D^\pm] = 1070 \pm 36$ fs (statistical error only) is consistent with present PDG average [4] $\tau[D^\pm] = 1051 \pm 13$ fs. The agreement with these precise measurements demonstrates our control of systematic effects. This $\tau[\Lambda_c^+]$ measurement has a total error that is a factor of 2 smaller than the best previously published result [11]. We look forward to measurements with similar precision of the lifetimes of the other 3 stable charmed baryons, by us and others, in the near future. The set of precision lifetime measurements required for a better understanding of charm weak decays should soon be available.

[a]Deceased.
[b]Present address: Infinion, München, Germany.
[c]Now at Imperial College, London SW7 2BZ, U.K.
[d]Now at Instituto de Física da Universidade Estadual de Campinas, UNICAMP, SP, Brazil.
[e]Now at Physik-Department, Technische Universität München, 5748 Garching, Germany.
[f]Present address: The Boston Consulting Group, München, Germany.
[g]Present address: Lucent Technologies, Naperville, IL.
[h]Now at Instituto de Física Teórica da Universidade Estadual Paulista, São Paulo, Brazil.
[i]Present address: SPSS Inc., Chicago, IL.
[j]Now at University of Alabama at Birmingham, Birmingham, AL 35294.
[k]Present address: DOE, Germantown, MD.
[l]Present address: Siemens Medizintechnik, Erlangen, Germany.
[m]Present address: Deutsche Bank AG, Eschborn, Germany.

[1] J. G. Körner and M. Krämer, Z. Phys. C **55**, 659 (1992).
[2] M. Bauer, B. Stech, and M. Wirbel, Z. Phys. C **34**, 103 (1987).
[3] G. Bellini, I. Bigi, and P. J. Dornan, Phys. Rep. **289**, 1 (1997), and references therein.
[4] Particle Data Group, D. E. Groom et al., Eur. Phys. J. C **15**, 1 (2000).
[5] SELEX Collaboration, J. S. Russ et al., in *Proceedings of the 29th International Conference on High Energy Physics, 1998,* edited by A. Astbury et al. (World Scientific, Singapore, 1998), Vol. II, p. 1259; hep-ex/9812031.
[6] A. Y. Kushnirenko, Ph.D. thesis, Carnegie Mellon University, 2000.
[7] J. Engelfried et al., Nucl. Instrum. Methods Phys. Res., Sect. A **431**, 53 (1999).
[8] P. L. Frabetti et al., Phys. Lett. B **323**, 459 (1994).
[9] E. M. Aitala et al., Phys. Rev. Lett. **83**, 32 (1999).
[10] G. Bonvicini et al., Phys. Rev. Lett. **82**, 4586 (1999).
[11] P. L. Frabetti et al., Phys. Rev. Lett. **70**, 1755 (1993).